Beamforming Cancellation Design for Millimeter-Wave Full-Duplex

Ian P. Roberts
University of Texas at Austin

Sriram Vishwanath
GenXComm, Inc., Austin, Texas, USA

***Abstract*—In recent years, there has been extensive research on millimeter-wave (mmWave) communication and on in-band full-duplex (FD) communication, but work on the combination of the two is relatively lacking. FD mmWave systems could offer increased spectral efficiency and decreased latency while also suggesting the redesign of existing mmWave applications. While FD technology has been well-explored for sub-6 GHz systems, the developed methods do not translate well to mmWave. This turns us to a method called beamforming cancellation (BFC), where the highly directional mmWave beams are steered to mitigate self-interference (SI) and enable simultaneous transmission and reception in-band. In this paper, we present BFC designs for two fully-connected hybrid beamforming scenarios, both of which sufficiently suppress the SI such that the sum spectral efficiency approaches that of a SI-free FD system. A simulation and its results are then used to verify our designs.**

I. Introduction

The revolution on millimeter-wave (mmWave) communication has enabled it to become a core technology of fifth generation (5G) cellular networks. The wide bandwidths available at mmWave make it an attractive choice for higher rates, but challenges remain in the design of communication systems at such high carrier frequencies [1], [2]. Due to its high path loss, mmWave communication necessitates the use of dense antenna arrays to provide sufficient beamforming gains to close the link and enough margin for wide-area use [2], [3].

In mmWave multiple-input multiple-output (MIMO) communication, it is not practical to have a dedicated radio frequency (RF) chain for each array element due to the associated financial cost, power consumption, size, and complexity [4]. Thus, hybrid analog/digital beamforming is often employed, where the combination of a baseband (digital) beamformer and a RF (analog) beamformer is used to achieve performance comparable to a fully-digital beamformer while reducing the number of RF chains [2], [4], [5].

First introduced about a decade ago, in-band full-duplex (FD) communication enables transmission and reception using the same time-frequency resource [6]. Such a capability offers exciting potential due to its possible doubling of spectral efficiency and the opportunity to reimagine applications that use conventional half-duplex (HD) techniques. To name a few, cognitive radio, relay nodes, and medium access control (MAC) are areas where the ability to simultaneously transmit and receive can introduce gains aside from increased spectral efficiency. When attempting to receive while transmitting, a device incurs self-interference (SI) which corrupts the desired receive signal if not dealt with. In order to achieve FD, researchers have developed various self-interference cancellation (SIC) methods, which take advantage of the fact that a transceiver is privy to its transmit signal, enabling it to reconstruct the SI and subtract it from the corrupted signal. This leaves the desired receive signal nearly interference-free if done properly.

The majority of existing work on FD, however, is in its application to sub-6 GHz systems. With the rise of mmWave and its role in 5G, the extension of FD to mmWave is of considerable interest. However, mmWave FD cannot be realized by simply applying the SIC methods developed for sub-6 GHz systems. This is largely due to the numerous antennas in use, wide bandwidths, increased phase noise, and highly nonlinear components at mmWave [7].

There has been introductory work on achieving mmWave FD using a technique known as beamforming cancellation (BFC), where the highly directional mmWave beams are used to mitigate SI by strategic steering [7], [8]. When operating in a FD fashion at mmWave, both a transmit and receive beamformer will be in use simultaneously and will operate over the same frequencies. The goal of BFC is to steer the transmit and receive beamformers such that they mitigate the SI while successfully transmitting to and receiving from the desired user(s).

Without BFC, the SI strength will likely be many orders of magnitude stronger than the incoming desired receive signal, meaning the beamformers must be designed to sufficiently mitigate the SI power while still providing sufficient gain on the desired links for successful communication. These requirements are especially true given that practical mmWave communication is typically at low signal-to-noise ratio (SNR).

The hybrid architectures used at mmWave complicate BFC due to the limitations of the analog beamformer and a desirably low number of RF chains. In this paper, we present two BFC designs where FD communication can be achieved at mmWave under two different fully-connected hybrid beamforming scenarios. We then present the results of simulation which validate our designs, both of which exhibit performance that can meet near ideal FD operation. Additionally, we show that eigen-beamformers alone do not sufficiently suppress the SI, even with the highly directional nature of mmWave beams.

Existing mmWave FD designs are limited in literature. Some designs, for example, do not consider SI at all in their work [9]. The few existing BFC designs that consider SI

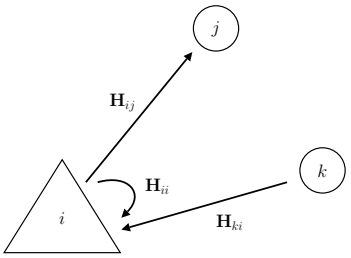

Fig. 1. A FD node (i) suffering from SI as it simultaneously transmits to (j) and receives from (k).

are iterative approaches that rely on convergence to a locally optimum solution and involve joint design across transmitter and receiver pairs [7], [10]. Our design, on the other hand, is not iterative and does not rely on a joint design across nodes. Additionally, our methods consider the hybrid structure and its limitations during design whereas existing approaches assume fully-digital beamforming and decompose into hybrid approximations after the fact, not necessarily considering limitations such as phase shifter resolution.

We use the following notation. We use bold uppercase, $\mathbf{A}$, to represent matrices. We use bold lowercase, $\mathbf{a}$, to represent column vectors. We use $(\cdot)^{\mathsf{T}}$, $(\cdot)^{\mathsf{H}}$, and $||\cdot||_{\mathsf{F}}$ to represent matrix transpose, conjugate transpose, and Frobenius norm, respectively. We use $[\mathbf{A}]_{i,j}$ to denote the element in the ith row and jth column of $\mathbf{A}$.

II. System Model

Before presenting our design, we provide preliminary information on the system model and our assumptions. Let us consider the mmWave network in Fig. 1 where a FD node (i) is simultaneously transmitting to HD node (j) and receiving from HD node (k) in the same frequency band.

We assume (i) has separate transmit and receive arrays so that it can realize two completely independent beamformers. We further assume node (i) employs fully-connected hybrid beamforming [2] where the RF beamformers are subject to a constant amplitude (CA) constraint whereby they have phase control but lack amplitude control. We assume nodes (j) and (k) can perfectly realize a fully-digital beamformer via hybrid beamforming (e.g., using [11]). Thus, we can ignore the hybrid architecture at (j) and (k).

We let the number of transmit antennas, N_{t}, and the number of receive antennas, N_{r}, be the same at all nodes for convenience of notation and in analysis. Since we are focusing on the hybrid architecture at (i), we let N_{RF} be the number of RF chains at its transmit array and at its receive array. At each node, we impose a per-symbol power constraint along with uniform power allocation across streams such that the Frobenius norm of each stream's precoder must be $\sqrt{N_{\mathrm{t}}}$.

Let $\mathbf{F}_{\mathrm{BB}}^{(i)}$, $\mathbf{F}_{\mathrm{RF}}^{(i)}$, $\mathbf{W}_{\mathrm{RF}}^{(i)}$, and $\mathbf{W}_{\mathrm{BB}}^{(i)}$ denote the baseband precoder, RF precoder, RF combiner, and baseband combiner, all at (i), respectively. Abiding by the CA constraint, the entries of $\mathbf{F}_{\mathrm{RF}}^{(i)}$ and $\mathbf{W}_{\mathrm{RF}}^{(i)}$ are required to have unit magnitude. Let $\mathbf{F}^{(k)}$ be the precoder at (k) and $\mathbf{W}^{(j)}$ be the combiner at (j).

Let $\mathbf{H}_{ki}$ be the $N_{\mathrm{r}} \times N_{\mathrm{t}}$ channel from (k) to (i). Let $\mathbf{H}_{ij}$ be the $N_{\mathrm{r}} \times N_{\mathrm{t}}$ channel from (i) to (j). Let $\mathbf{H}_{ii}$ be the $N_{\mathrm{r}} \times N_{\mathrm{t}}$ SI channel from the transmit array of (i) to its own receive array. Let $\mathbf{s}^{(i)} \sim \mathcal{N}_{\mathbb{C}}(\mathbf{0}, \mathbf{I})$ and $\mathbf{s}^{(j)} \sim \mathcal{N}_{\mathbb{C}}(\mathbf{0}, \mathbf{I})$ be the $N_{\mathrm{s}} \times 1$ symbol vectors intended for (i) and (j), respectively, where we have assumed the same number of streams is being sent on both links (and that each node has support of N_{s} streams). Let $\mathbf{n}^{(i)} \sim \mathcal{N}_{\mathbb{C}}(\mathbf{0}, \mathbf{I})$ and $\mathbf{n}^{(j)} \sim \mathcal{N}_{\mathbb{C}}(\mathbf{0}, \mathbf{I})$ be $N_{\mathrm{r}} \times 1$ noise vectors at the receive arrays of (i) and (j), respectively.

We define the SNR for a given link as accounting for transmit power and the link's path loss. Let SNR_{ki} and SNR_{ij} be the SNR from (k) to (i) and from (i) to (j), respectively. Let SNR_{ii} be the SNR of the SI.

Let us focus our attention on the FD node (i). We can represent its estimated receive symbol $\hat{\mathbf{s}}^{(i)}$ as follows, where (1) is the desired term, (2) is the resulting SI term, and (3) is the resulting noise term.

$$\hat{\mathbf{s}}^{(i)} = \sqrt{\mathsf{SNR}_{ki}}\, \mathbf{W}_{\mathrm{BB}}^{\mathsf{H}(i)} \mathbf{W}_{\mathrm{RF}}^{\mathsf{H}(i)} \mathbf{H}_{ki} \mathbf{F}^{(k)} \mathbf{s}^{(i)} \quad (1)$$

$$+ \sqrt{\mathsf{SNR}_{ii}}\, \mathbf{W}_{\mathrm{BB}}^{\mathsf{H}(i)} \mathbf{W}_{\mathrm{RF}}^{\mathsf{H}(i)} \mathbf{H}_{ii} \mathbf{F}_{\mathrm{RF}}^{(i)} \mathbf{F}_{\mathrm{BB}}^{(i)} \mathbf{s}^{(j)} \quad (2)$$

$$+ \mathbf{W}_{\mathrm{BB}}^{\mathsf{H}(i)} \mathbf{W}_{\mathrm{RF}}^{\mathsf{H}(i)} \mathbf{n}^{(i)} \quad (3)$$

As indicated by (2), the transmitted signal from (i) intended for (j) traverses through the SI channel $\mathbf{H}_{ii}$ and is received by the combiner at (i) being used for reception from (k).

The estimated receive symbol at (j) from (i) is

$$\hat{\mathbf{s}}^{(j)} = \sqrt{\mathsf{SNR}_{ij}}\, \mathbf{W}^{\mathsf{H}(j)} \mathbf{H}_{ij} \mathbf{F}_{\mathrm{RF}}^{(i)} \mathbf{F}_{\mathrm{BB}}^{(i)} \mathbf{s}^{(j)} + \mathbf{W}^{\mathsf{H}(j)} \mathbf{n}^{(j)}, \quad (4)$$

where (j) does not encounter any SI since it is a HD device. Additionally, we assume that there is no adjacent user interference between (j) and (k). We justify this assumption with the high path loss and directionality of transmission and reception at mmWave.

For the desired link channels, $\mathbf{H}_{ij}$ and $\mathbf{H}_{ki}$, we assume sufficient far-field conditions have been met. We employ the extended Saleh-Valenzuela mmWave channel representation as shown in (5). In this model, an $N_{\mathrm{r}} \times N_{\mathrm{t}}$ channel is the sum of the contributions from N_{clust} scattering clusters, each of which contributes N_{rays} propagation paths [4].

$$\mathbf{H} = \sqrt{\frac{N_{\mathrm{t}} N_{\mathrm{r}}}{N_{\mathsf{rays}} N_{\mathsf{clust}}}} \sum_{m=1}^{N_{\mathsf{clust}}} \sum_{n=1}^{N_{\mathsf{rays}}} \beta_{m,n} \mathbf{a}_{\mathrm{r}}(\theta_{m,n}) \mathbf{a}_{\mathrm{t}}^{\mathsf{H}}(\phi_{m,n}) \quad (5)$$

In (5), $\mathbf{a}_{\mathrm{r}}(\theta_{m,n})$ and $\mathbf{a}_{\mathrm{t}}(\phi_{m,n})$ are the antenna array responses at the receiver and transmitter, respectively, for ray n within cluster m which has some angle of arrival (AoA), $\theta_{m,n}$, and angle of departure (AoD), $\phi_{m,n}$. Each ray has a random gain $\beta_{m,n} \sim \mathcal{N}_{\mathbb{C}}(0, 1)$. The coefficient outside the summations is used to ensure that $\mathbb{E}\left[||\mathbf{H}||_{\mathsf{F}}^2\right] = N_{\mathrm{t}} N_{\mathrm{r}}$. Note that we have considered a single angular dimension (e.g., azimuth) for the AoAs and AoDs for simplicity and to agree with our use of uniform linear arrays (ULAs) in simulation.

When (i) transmits to (j) while receiving from (k), there will almost certainly be some undesired leakage from the transmit array to the receive array that corrupts the desired

receive signal. The strength of this leakage is a function of the precoder at (i), the combiner at (i), and the channel between them. The transmit and receive arrays at (i) will be relatively close together, meaning the far-field condition is not met and near-field effects must be considered. Unfortunately, the mmWave SI channel is much less understood since research and measurements at mmWave have primarily focused on more practical far-field scenarios. Therefore, we have turned to one of the few attempts at characterizing the mmWave SI channel [7], where it is decomposed in a Rician fashion containing a near-field line-of-sight (LOS) component and a far-field component stemming from non-line-of-sight (NLOS) reflections. Explicitly, we model the SI as

$$\mathbf{H}_{ii} = \sqrt{\frac{\kappa}{\kappa+1}}\mathbf{H}_{ii}^{\text{LOS}} + \sqrt{\frac{1}{\kappa+1}}\mathbf{H}_{ii}^{\text{NLOS}} \tag{6}$$

where κ is the Rician factor. The entries of the LOS contribution are modeled as [12]

$$\left[\mathbf{H}_{ii}^{\text{LOS}}\right]_{m,n} = \frac{\rho}{r_{m,n}} \exp\left(-\text{j}2\pi\frac{r_{m,n}}{\lambda_c}\right) \tag{7}$$

where ρ is a normalization constant such that $\mathbb{E}\left[||\mathbf{H}_{ii}||_{\text{F}}^2\right] = N_{\text{t}}N_{\text{r}}$ and $r_{m,n}$ is the distance from the mth element of the transmit array to the nth element of the receive array. We leave the definition of $r_{m,n}$ to [12] for space considerations. For the NLOS SI channel, we use the model in (5).

III. Proposed Beamforming Cancellation Designs

In order for (i) to simultaneously transmit and receive in-band, we seek to mitigate the SI by design of its transmit and/or receive beamformers. Performance on the desired links must be maintained to some degree or else transmission and reception will be poor. We assume (i) and (j) have perfect channel state information (CSI) of $\mathbf{H}_{ij}$ and that (k) and (i) have perfect CSI of $\mathbf{H}_{ki}$. We assume (i) also has perfect CSI of its SI channel, $\mathbf{H}_{ii}$.

To begin the design, we set $\mathbf{F}^{(k)}$ and $\mathbf{W}^{(j)}$ to be the so-called eigen-beamformers for their respective channels as follows. Taking the singular value decomposition (SVD) of $\mathbf{H}_{ki}$ and of $\mathbf{H}_{ij}$, we get

$$\mathbf{H}_{ki} = \mathbf{U}_{ki}\mathbf{\Sigma}_{ki}\mathbf{V}_{ki}^{\text{H}} \tag{8}$$

$$\mathbf{H}_{ij} = \mathbf{U}_{ij}\mathbf{\Sigma}_{ij}\mathbf{V}_{ij}^{\text{H}} \tag{9}$$

where $\mathbf{\Sigma}_{ki}$ and $\mathbf{\Sigma}_{ij}$ contain decreasing singular values along their diagonals. Setting $\mathbf{F}^{(k)}$ and $\mathbf{W}^{(j)}$ as the singular vectors corresponding to the N_{s} strongest eigenchannels, we have

$$\mathbf{F}^{(k)} = [\mathbf{V}_{ki}]_{:,0:N_{\text{s}}-1} \tag{10}$$

$$\mathbf{W}^{(j)} = [\mathbf{U}_{ij}]_{:,0:N_{\text{s}}-1} \tag{11}$$

where we use $[\cdot]_{:,0:N_{\text{s}}-1}$ to denote selecting the N_{s} leftmost columns. Abiding by our power constraint, (10) is normalized such that its columns have Frobenius norm $\sqrt{N_{\text{t}}}$. We have assumed (k) and (j) can perfectly realize these fully-digital beamformers. Furthermore, having assumed perfect CSI implies that (i) has knowledge of $\mathbf{F}^{(k)}$ and $\mathbf{W}^{(j)}$.

Since (i) employs hybrid beamforming, constructing a desired beamformer occurs in an analog stage and a digital stage. The analog beamformer and the number of RF chains impose limitations on the accuracy of the hybrid construction. For this reason, we explore two scenarios based on the hybrid architecture in use. The first is a less practical case when the hybrid beamformers have infinite precision phase shifters and twice the number of RF chains as streams, i.e., $N_{\text{RF}} = 2N_{\text{s}}$. In the second scenario, we consider a more practical hybrid architecture where $2N_{\text{s}} > N_{\text{RF}} \geq N_{\text{s}}$ and the phase shifters have finite resolution. In both cases, we assume the analog beamformers abide by the CA constraint and that fully-connected hybrid beamforming is employed.

Case A: $N_{RF} = 2N_s$ & Infinite Resolution Phase Shifters

In this scenario, we assume that the phase shifters have infinite precision and that there are twice as many RF chains as there are streams. Given these assumptions, we reference the work of [11] where it was shown that having $N_{\text{RF}} = 2N_{\text{s}}$ and infinite precision phase shifters enables perfect hybrid decomposition of any fully-digital beamformer. This alleviates our BFC design in Case A of any hybrid architectural constraints and allows us to decompose a fully-digital design without penalty.

To begin our design, we first choose the fully-digital combiner at (i), $\mathbf{W}^{(i)}$, to be the eigen-combiner for its link with (k). Using (8), we get

$$\mathbf{W}^{(i)} = [\mathbf{U}_{ki}]_{:,0:N_{\text{s}}-1}\,. \tag{12}$$

Choosing to fix $\mathbf{W}^{(i)}$ allows us to consider the *effective* SI channel, which is the portion of the SI channel that gets received by the combiner at (i) as it receives from (k). This effective SI channel is then

$$\mathbf{W}^{\text{H}(i)}\mathbf{H}_{ii}. \tag{13}$$

Ideally, our choice for $\mathbf{F}^{(i)}$ would be such that it contributes no SI while transmitting to (j). Put simply, we desire

$$\mathbf{W}^{\text{H}(i)}\mathbf{H}_{ii}\mathbf{F}^{(i)} = \mathbf{0}. \tag{14}$$

Setting $\mathbf{F}^{(i)}$ to the eigen-precoder, however, would very likely violate (14), introducing SI, corrupting the signal from (k), and degrading the spectral efficiency of its link with (k). The eigen-precoder and eigen-combiner would satisfy (14) only if they happened to be orthogonal.

Fixing $\mathbf{W}^{(i)}$, for (14) to hold, $\mathbf{F}^{(i)}$ must lie in the null space of $\mathbf{W}^{\text{H}(i)}\mathbf{H}_{ii}$. An alternate interpretation as to why we have chosen to consider the effective SI channel rather than the entire SI channel is as follows. The SI channel model we have employed in (6) and (7) is full rank, leaving no dimensions for the null space by the rank-nullity theorem. This has inspired us to more appropriately consider the effective SI channel in (13) rather than solely $\mathbf{H}_{ii}$, leaving a null space with many dimensions for $\mathbf{F}^{(i)}$ to live. In short, we only need to be concerned with the portion of SI that is *received*.

Since it is likely that the eigen-precoder will not naturally lie in the null space of the effective SI channel, we seek to project it as follows. Let $\mathbf{B} = \text{null}\left(\mathbf{W}^{\mathsf{H}^{(i)}}\mathbf{H}_{ii}\right)$ be a matrix whose columns are a basis of the null space of the effective SI channel. The matrix $\mathbf{B}$ can be found in multiple ways, a simple one being comprised of the right singular vectors of the effective SI channel that correspond to singular values of zero. The projection matrix for the column space of $\mathbf{B}$ is then

$$\mathbf{P} = \mathbf{B}\left(\mathbf{B}^{\mathsf{H}}\mathbf{B}\right)^{-1}\mathbf{B}^{\mathsf{H}} \tag{15}$$

which is used to project the eigen-precoder onto $\mathbf{B}$ by

$$\mathbf{F}^{(i)} = \mathbf{P}\left[\mathbf{V}_{ij}\right]_{:,0:N_{\text{s}}-1} \tag{16}$$

where $\mathbf{V}_{ij}$ are the right singular vectors from (9). Abiding by our power constraint, (16) is normalized such that its columns have Frobenius norm $\sqrt{N_{\text{t}}}$.

Given this scenario's hybrid assumptions, we invoke the method in [11] for determining the analog and digital beamformers that perfectly construct the desired fully-digital beamformers $\mathbf{F}^{(i)}$ and $\mathbf{W}^{(i)}$ in a hybrid fashion.

Case B: $2N_s > N_{RF} \geq N_s$ & Finite Resolution Phase Shifters

In this scenario, we consider more practical implementation conditions, where the number of RF chains is less than twice the number of streams, $2N_{\text{s}} > N_{\text{RF}} \geq N_{\text{s}}$, and the phase shifters have finite resolution. Our design does not rely on a specific phase shifter resolution, though higher resolution phase shifters will naturally yield better performance.

A popular and effective hybrid decomposition algorithm for such a scenario uses orthogonal matching pursuit (OMP) to decompose a desired fully-digital beamformer into its hybrid counterpart by capturing the analog limitations in an analog beamforming codebook [13]. We cannot directly apply this OMP-based decomposition to the fully-digital solution found in Case A, however, since the hybrid approximation of $\mathbf{F}^{(i)}$ will not necessarily lie in the null space of the effective SI channel—orthogonality is likely lost during hybrid approximation. Instead, our method for this case projects $\mathbf{F}^{(i)}$ into the null space of the effective SI channel *during* hybrid decomposition, rather than before as in Case A. Our design is as follows.

We first choose $\mathbf{W}^{(i)}$ to be the eigen-combiner for its link with (k) as shown in (12). Since we are considering the aforementioned practical limitations, we must approximate this fully-digital beamformer by its hybrid counterpart. We choose to perform this hybrid decomposition before proceeding rather than later as will be apparent. The hybrid approximation of $\mathbf{W}^{(i)}$ can be done using the OMP-based approach, for example, though our design does not require a particular hybrid decomposition method for the combiner. Following hybrid approximation, the effective combiner at (i) is $\mathbf{W}_{\text{RF}}^{(i)}\mathbf{W}_{\text{BB}}^{(i)}$.

We begin the design of $\mathbf{F}^{(i)}$ by initializing it to the eigen-precoder

$$\mathbf{F}^{(i)} = \left[\mathbf{V}_{ij}\right]_{:,0:N_{\text{s}}-1}. \tag{17}$$

Let $\mathbf{A}_{\text{RF}}$ be a matrix whose columns are valid analog beamforming vectors. We invoke a conventional OMP-based hybrid approximation of $\mathbf{F}^{(i)}$ using $\mathbf{A}_{\text{RF}}$ which returns an analog precoder $\mathbf{X}_{\text{RF}}$ and a digital precoder $\mathbf{X}_{\text{BB}}$ whose product approximates the eigen-precoder and meets the hybrid constraints.

To ensure that there is no leakage of a transmission into the receive array and since the analog precoder is limited by its constraints, we project the digital precoder into the null space of the effective SI channel (18). Thus, we set the analog beamformer as $\mathbf{F}_{\text{RF}}^{(i)} = \mathbf{X}_{\text{RF}}$ and focus only on the digital beamformer.

Having set the hybrid combiner to $\mathbf{W}_{\text{RF}}^{(i)}\mathbf{W}_{\text{BB}}^{(i)}$ and the analog precoder to $\mathbf{F}_{\text{RF}}^{(i)}$, the effective SI channel becomes

$$\mathbf{W}_{\text{BB}}^{\mathsf{H}^{(i)}}\mathbf{W}_{\text{RF}}^{\mathsf{H}^{(i)}}\mathbf{H}_{ii}\mathbf{F}_{\text{RF}}^{(i)}. \tag{18}$$

Let $\mathbf{C} = \text{null}\left(\mathbf{W}_{\text{BB}}^{\mathsf{H}^{(i)}}\mathbf{W}_{\text{RF}}^{\mathsf{H}^{(i)}}\mathbf{H}_{ii}\mathbf{F}_{\text{RF}}^{(i)}\right)$ be a matrix whose columns are a basis of the null space of the effective SI channel in (18). The projection matrix for $\mathbf{C}$ is

$$\mathbf{Q} = \mathbf{C}\left(\mathbf{C}^{\mathsf{H}}\mathbf{C}\right)^{-1}\mathbf{C}^{\mathsf{H}}. \tag{19}$$

which is used to project the digital precoder $\mathbf{X}_{\text{BB}}$ onto the column space of $\mathbf{C}$ by

$$\mathbf{F}_{\text{BB}}^{(i)} = \mathbf{Q}\mathbf{X}_{\text{BB}}. \tag{20}$$

The effective precoder at (i) is then

$$\mathbf{F}^{(i)} = \mathbf{F}_{\text{RF}}^{(i)}\mathbf{F}_{\text{BB}}^{(i)} = \mathbf{X}_{\text{RF}}\mathbf{Q}\mathbf{X}_{\text{BB}} \tag{21}$$

which is normalized such that its columns have Frobenius norm $\sqrt{N_{\text{t}}}$. This concludes our design, which we validate in the next section using simulation. In both designs, for Case A and Case B, our transmit precoder is designed such that reception from (k) is unaffected by transmission to (j).

IV. Simulation and Results

In order to verify our proposed method, a simulation was developed in MATLAB. We denote the carrier wavelength as λ_{c}. We assume all antenna arrays to be ULAs with element spacing $\lambda_{\text{c}}/2$. Each array element is assumed to be isotropic. The array response vector can be formulated as $\mathbf{a}(\theta) = \left[1\ e^{\mathrm{j}\varphi(\theta)}\ e^{\mathrm{j}2\varphi(\theta)}\ \ldots\ e^{\mathrm{j}(N_{\text{a}}-1)\varphi(\theta)}\right]^{\mathsf{T}}$ where N_{a} is the number of elements in the array and $\varphi(\theta) = \frac{2\pi}{\lambda_{\text{c}}}\frac{\lambda_{\text{c}}}{2}\cos(\theta)$ is the phase shift between elements.

For generating the channels $\mathbf{H}_{ki}$ and $\mathbf{H}_{ij}$, we use a random number of clusters and rays per cluster uniformly distributed on $[1, 6]$ and $[1, 10]$, respectively. Within a given cluster, each ray's AoD and AoA are Laplacian distributed sharing a mean which is uniformly distributed on $[0, \pi]$ and having standard deviation of 0.2.

The SI Rician factor is chosen to be $\kappa = 30$ dB, since we assume the LOS SI would dominate in practice. We assume the transmit and receive arrays at (i) are separated by a distance $10\lambda_{\text{c}}$ and an angle $\pi/6$. For generating $\mathbf{H}_{ii}^{\text{NLOS}}$, we do so in the same fashion as the desired links $\mathbf{H}_{ki}$ and $\mathbf{H}_{ij}$ but having

a random number of clusters and rays uniformly distributed on $[1, 3]$ and $[1, 3]$, since we assume there would be less scattering due to the close proximity. The SI SNR is set to be $\mathsf{SNR}_{ii} = 120$ dB where we have imagined a practical scenario having a SI power of 30 dBm at the receive array and a noise floor of -90 dBm. We let the link SNRs from (k) to (i) and from (i) to (j) to be equal for the sake of interpreting the results, i.e., $\mathsf{SNR}_{ki} = \mathsf{SNR}_{ij} = \mathsf{SNR}$.

Results of Case A

Having infinite precision phase shifters and $N_{\text{RF}} = 2N_{\text{s}}$, we can perfectly replicate our design for Case A using hybrid beamforming. In Fig. 2 and Fig. 3, we compare various spectral efficiencies for $N_{\text{t}} = N_{\text{r}} = 16$ and $N_{\text{t}} = N_{\text{r}} = 64$, respectively, where $N_{\text{s}} = 3$ in both.

When using its eigen-precoder and eigen-combiner, (i) will almost certainly collect some portion of SI. Since the SI is extremely strong relative to a desired receive signal, even a small fraction of SI overwhelms the desired receive signal, making successful reception from (k) nearly impossible. Transmission to (j) is not impacted since we are using the eigen-precoder and (j) is unaffected by the SI at (i). This results in a spectral efficiency to (j) equivalent to its HD spectral efficiency and a spectral efficiency from (k) being practically zero due to the dominating SI. Thus, the sum spectral efficiency using eigen-beamforming at (i) is nearly identical to the HD case where only a single node, (i) or (k), transmits. These results indicate that eigen-beamforming is not sufficient for FD operation even at mmWave where the beams are highly directional.

With our BFC design, however, the sum spectral efficiency hugs the ideal FD spectral efficiency curve quite closely. Ideal FD operation is simply the case when the degrading effects of SI are not present, allowing both HD links to operate at their maximum rates simultaneously. By design, we completely eliminate the received SI, allowing the link from (k) to achieve a spectral efficiency equal to its HD spectral efficiency even while (j) is simultaneously being served. The spectral efficiency of the link from (i) to (j) is slightly degraded compared to during HD operation due to $\mathbf{F}^{(i)}$ deviating from the eigen-precoder as it is projected into the null space of the effective SI—this is the only cost of operating in FD with our BFC design. The ability to perfectly recreate our fully-digital beamformers in a hybrid fashion in this scenario allows us to attribute any deviation from ideal FD performance to our design and not to the hybrid approximation.

When 64 antennas are in use, there are two important factors at play. The first is that higher spectral efficiencies can be achieved at a given link SNR compared to with 16 antennas, of course, due to the increased beamforming gain. The second factor is that, with more antennas but constant N_{s}, our null space dimension grows, allowing us to more accurately approximate our eigen-precoder while constraining it to live in the null space of the effective SI.

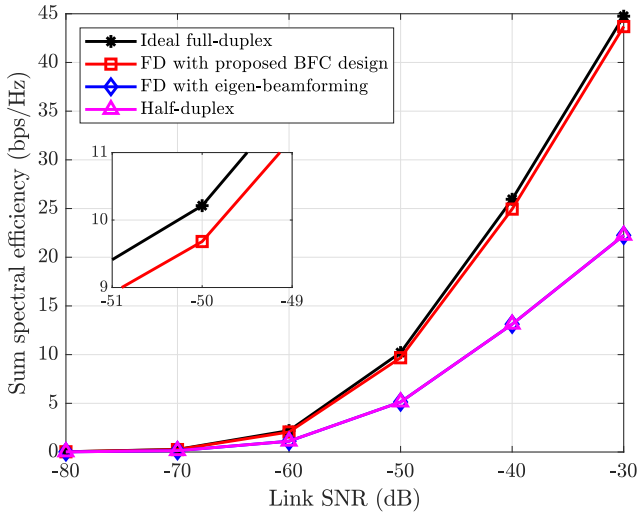

Fig. 2. Sum spectral efficiencies achieved with infinite precision phase shifters when $N_{\text{s}} = 3$, $N_{\text{RF}} = 6$, and $N_{\text{t}} = N_{\text{r}} = 16$.

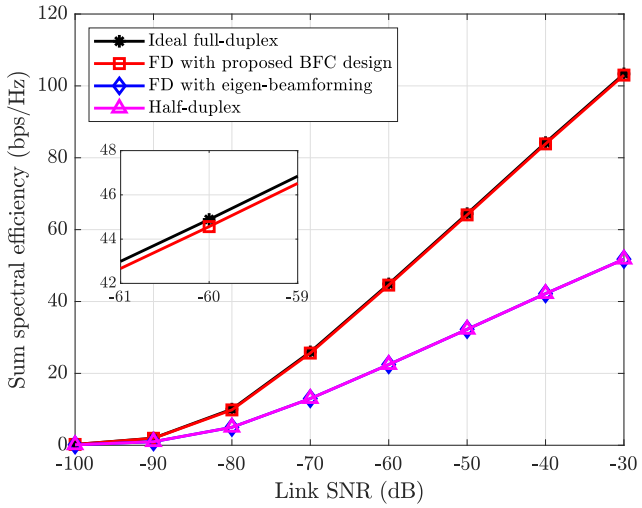

Fig. 3. Sum spectral efficiencies achieved with infinite precision phase shifters when $N_{\text{s}} = 3$, $N_{\text{RF}} = 6$, and $N_{\text{t}} = N_{\text{r}} = 64$.

Results of Case B

For the scenario where we have finite precision phase shifters and $2N_{\text{s}} > N_{\text{RF}} \geq N_{\text{s}}$, we have used OMP-based hybrid approximation which uses a codebook for choosing analog beamformers that satisfy the CA constraint and phase shifter resolution. For simulation, we have used a discrete Fourier transform (DFT) analog beamforming codebook, which does not contain anywhere near every possible analog beamformer meaning it could result in sub-optimality. However, since we have taken this scenario to be a practical one, using the DFT codebook is deemed a suitable choice for its computational convenience and sufficient performance with ULAs. It is worth noting that this choice implicitly assumes that our phase shifters have a resolution of at least $2\pi/N_{\text{a}}$, where N_{a} is the number of antennas at the beamformer. In general, an appropriate beamforming codebook should be

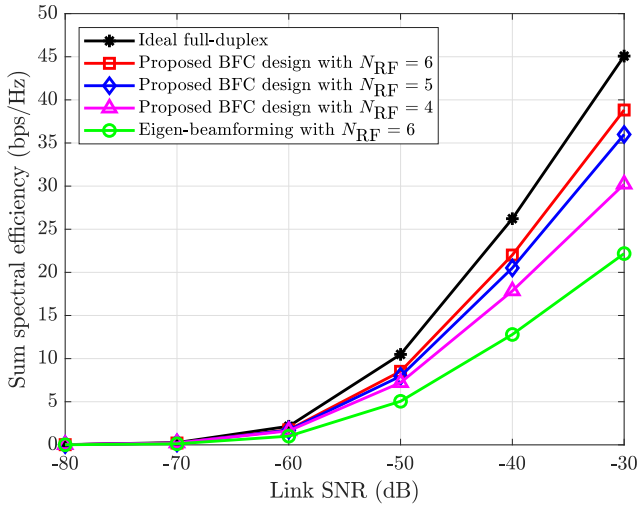

Fig. 4. Sum spectral efficiency for varying number of RF chains with finite resolution phase shifters when $N_{\mathrm{s}} = 3$ and $N_{\mathrm{t}} = N_{\mathrm{r}} = 16$.

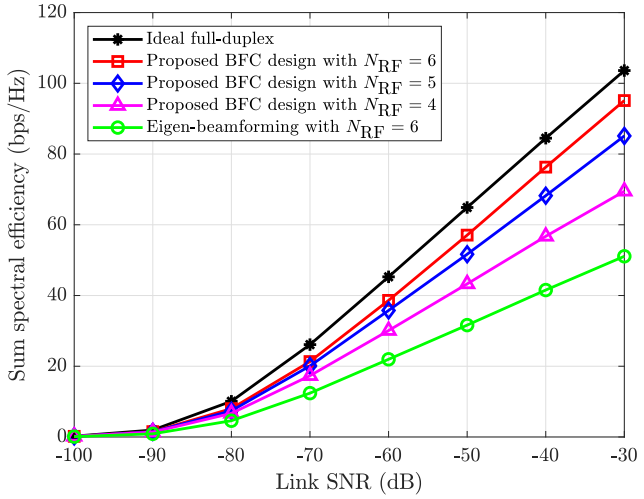

Fig. 5. Sum spectral efficiency for varying number of RF chains with finite resolution phase shifters when $N_{\mathrm{s}} = 3$ and $N_{\mathrm{t}} = N_{\mathrm{r}} = 64$.

chosen based on the particular analog beamformer's limitations. Given this sub-optimality, we will observe some loss during projection into the null space in addition to the loss during hybrid approximation. We have observed, however, that the loss during hybrid approximation is fairly insignificant, especially with increasing N_{RF}.

As seen in Fig. 4 and Fig. 5, our BFC design incorporating the hybrid architectural constraints performs quite well, especially for an increasing number of RF chains. In both figures, we let $N_{\mathrm{s}} = 3$ and vary the number of RF chains. With $N_{\mathrm{RF}} \geq 4$, we see that our BFC design outperforms the hybrid-approximated eigen-precoder having $N_{\mathrm{RF}} = 6$, netting a higher sum spectral efficiency. This increase in sum spectral efficiency is attributed to increased performance on the link from (i) to (j), primarily due to more closely approaching the eigen-precoder while projecting it into the null space of the effective SI channel. In other words, increasing the number of RF chains allows us to suppress the SI while better transmitting to (j) by offering more dimensions to the digital precoder $\mathbf{F}_{\mathrm{BB}}^{(i)}$. Our observations attribute only marginal gain to improved hybrid approximation as N_{RF} increases—the spectral efficiency gains are primarily due to improved BFC.

V. Conclusion

In this paper, we have presented beamforming designs for mmWave FD, enabling simultaneous transmission and reception in-band. Accounting for the hybrid architectures used at mmWave, we have proposed two designs: one for a more design-favorable scenario and another for a more practical one. In both, we abide by a CA constraint at the analog beamformers and employ a fully-connected hybrid architecture. We show that a device using our designs can achieve significant spectral efficiency gains approaching that of ideal FD operation. Our results indicate that mmWave FD applications can be enabled by our designs, offering increased spectral efficiency with the ability to transmit while receiving, even under the constraints imposed by hybrid beamforming.

References

[1] J. G. Andrews, S. Buzzi, W. Choi, S. V. Hanly, A. Lozano, A. C. K. Soong, and J. C. Zhang, "What will 5G be?" *IEEE Journal on Selected Areas in Communications*, vol. 32, no. 6, pp. 1065–1082, Jun 2014.

[2] R. W. Heath, N. Gonzalez-Prelcic, S. Rangan, W. Roh, and A. M. Sayeed, "An overview of signal processing techniques for millimeter wave MIMO systems," *IEEE Journal of Selected Topics in Signal Processing*, vol. 10, no. 3, pp. 436–453, Apr. 2016.

[3] R. W. Heath Jr. and A. Lozano, *Foundations of MIMO Communication*. Cambridge University Press, 2018.

[4] R. Mendez-Rial, C. Rusu, N. Gonzalez-Prelcic, A. Alkhateeb, and R. W. Heath, "Hybrid MIMO architectures for millimeter wave communications: Phase shifters or switches?" *IEEE Access*, vol. 4, pp. 247–267, 2016.

[5] S. Sun, T. Rappaport, R. Heath, A. Nix, and S. Rangan, "MIMO for millimeter-wave wireless communications: beamforming, spatial multiplexing, or both?" *IEEE Communications Magazine*, vol. 52, no. 12, pp. 110–121, Dec. 2014.

[6] J. I. Choi, M. Jain, K. Srinivasan, P. Levis, and S. Katti, "Achieving single channel, full duplex wireless communication," in *Proceedings of the 16th annual international conference on mobile computing and networking*. ACM, 2010, pp. 1–12.

[7] K. Satyanarayana, *et al.*, "Hybrid beamforming design for full-duplex millimeter wave communication," *IEEE Transactions on Vehicular Technology*, vol. 68, no. 2, pp. 1394–1404, Feb. 2019.

[8] Z. Xiao, P. Xia, and X. Xia, "Full-duplex millimeter-wave communication," *IEEE Wireless Communications*, vol. 24, no. 6, pp. 136–143, Dec. 2017.

[9] H. Abbas and K. Hamdi, "Full duplex relay in millimeter wave backhaul links," in *IEEE Wireless Communications and Networking Conference*, Apr 2016, pp. 1–6.

[10] D. Jagyasi and P. Ubaidulla, "In-band full-duplex relay-assisted millimeter-wave system design," *IEEE Access*, vol. 7, pp. 2291–2304, 2019.

[11] F. Sohrabi and W. Yu, "Hybrid digital and analog beamforming design for large-scale antenna arrays," *IEEE Journal of Selected Topics in Signal Processing*, vol. 10, no. 3, pp. 501–513, Apr. 2016.

[12] J. S. Jiang and M. A. Ingram, "Spherical-wave model for short-range MIMO," *IEEE Transactions on Communications*, vol. 53, no. 9, pp. 1534–1541, Sep. 2005.

[13] O. E. Ayach, S. Rajagopal, S. Abu-Surra, Z. Pi, and R. W. Heath, "Spatially sparse precoding in millimeter wave MIMO systems," *IEEE Transactions on Wireless Communications*, vol. 13, no. 3, pp. 1499–1513, Mar. 2014.